Mineralogical Magazine (2019), **83**, 107–113
doi:10.1180/minmag.2017.081.102

CAMBRIDGE UNIVERSITY PRESS

Article

Hydroxynatropyrochlore, $(Na,Ca,Ce)_2Nb_2O_6(OH)$, a new member of the pyrochlore group from the Kovdor phoscorite–carbonatite pipe, Kola Peninsula, Russia

Gregory Yu. Ivanyuk[1], Victor N. Yakovenchuk[1], Taras L. Panikorovskii[1,2], Nataliya Konoplyova[1], Yakov A. Pakhomovsky[1], Ayya V. Bazai[1], Vladimir N. Bocharov[3] and Sergey V. Krivovichev[1,2]

[1]Kola Science Centre, Russian Academy of Sciences, 14 Fersman Street, Apatity 184200, Russia; [2]Department of Crystallography, St. Petersburg State University, 7–9 University Emb, St. Petersburg 199034, Russia; and [3]Geo Environmental Centre "Geomodel", St. Petersburg State University, Ul'yanovskaya Str., St. Petersburg 198504, Russia

Abstract

Hydroxynatropyrochlore, $(Na,Ca,Ce)_2Nb_2O_6(OH)$, is a new Na–Nb–OH-dominant member of the pyrochlore supergroup from the Kovdor phoscorite–carbonatite pipe, Kola Peninsula, Russia. It is cubic, $Fd\bar{3}m$, $a = 10.3211(3)$ Å, $V = 1099.46(8)$ Å^3 and $Z = 8$ (from powder diffraction data) or $a = 10.3276(5)$ Å, $V = 1101.5(2)$ Å^3 and $Z = 8$ (from single-crystal diffraction data). Hydroxynatropyrochlore is a characteristic accessory mineral of the low-carbonate phoscorite in the contact zone of the phoscorite–carbonatite pipe with host foidolite as well as in the carbonate-rich phoscorite and carbonatite of the pipe axial zone. It usually forms zonal cubic or cubooctahedral crystals (up to 0.5 mm in diameter) with irregularly shaped relics of amorphous U–Ta-rich hydroxykenopyrochlore inside. Characteristic associated minerals include rock-forming calcite, dolomite, forsterite, hydroxylapatite, magnetite and phlogopite, accessory baddeleyite, baryte, barytocalcite, chalcopyrite, chamosite–clinochlore, galena, gladiusite, juonniite, ilmenite, magnesite, pyrite, pyrrhotite, quintinite, spinel, strontianite, valleriite and zirconolite. Hydroxynatropyrochlore is pale brown, with an adamantine to greasy lustre and a white streak. The cleavage is average on {111} and the fracture is conchoidal. Mohs hardness is ~5. In transmitted light, the mineral is light brown, isotropic and $n = 2.10(5)$ ($\lambda = 589$ nm). The calculated and measured densities are 4.77 and 4.60(5) g cm^{-3}, respectively. The mean chemical composition determined by electron microprobe is: F 0.05, Na_2O 7.97, CaO 10.38, TiO_2 4.71, FeO 0.42, Nb_2O_5 56.44, Ce_2O_3 3.56, Ta_2O_5 4.73, ThO_2 5.73, UO_2 3.66, total 97.65 wt.%. The empirical formula calculated on the basis of Nb + Ta + Ti = 2 apfu is $(Na_{1.02}Ca_{0.73}Ce_{0.09}Th_{0.09}U_{0.05}Fe^{2+}_{0.02})_{\Sigma 2.00}(Nb_{1.68}Ti_{0.23}Ta_{0.09})_{\Sigma 2.00}O_{6.03}(OH_{1.04}F_{0.01})_{\Sigma 1.05}$. The simplified formula is $(Na,Ca,Ce)_2Nb_2O_6(OH)$. The mineral dissolves slowly in hot HCl. The strongest X-ray powder-diffraction lines [listed as (d in Å)(I)(hkl)] are as follows: 5.96(47)(111), 3.110(30)(311), 2.580(100)(222), 2.368(19)(400), 1.9875(6)(333), 1.8257(25)(440) and 1.5561(14)(622). The crystal structure of hydroxynatropyrochlore was refined to $R_1 = 0.026$ on the basis of 80 unique observed reflections. The mineral belongs to the pyrochlore structure type $A_2B_2O_6Y_1$ with octahedral framework of corner-sharing BO_6 octahedra with A cations and OH groups in the interstices. The Raman spectrum of hydroxynatropyrochlore contains characteristic bands of the lattice, BO_6, B–O and O–H vibrations and no characteristic bands of the H_2O vibrations. Within the Kovdor phoscorite–carbonatite pipe, hydroxynatropyrochlore is the latest hydrothermal mineral of the pyrochlore supergroup, which forms external rims around grains of earlier U-rich hydroxykenopyrochlore and separated crystals in voids of dolomite carbonatite veins. The mineral is named in accordance with the pyrochlore supergroup nomenclature.

Keywords: hydroxynatropyrochlore, new mineral, sodium-calcium niobate, phoscorite, carbonatite, Kovdor

(Received 5 November 2017; accepted 19 December 2017)

Introduction

Minerals of the pyrochlore supergroup have recently attracted considerable attention and several new members of the group have been described from various world localities (Atencio *et al.*, 2010, 2013, 2017; Witzke *et al.*, 2011; Christy and Atencio, 2013; Biagioni *et al.*, 2013; Hålenius and Bosi, 2013; Yang *et al.*, 2014; Jingwu *et al.*, 2015; Andrade *et al.*, 2013, 2015, 2016; Li *et al.*, 2016; Fan *et al.*, 2016; Mills *et al.*, 2017). The pyrochlore-supergroup minerals are abundant in the Kovdor phoscorite-carbonatite pipe (Ivanyuk *et al.*, 2002, 2016; Mikhailova *et al.*, 2016; Kalashnikov *et al.*, 2016), with an economic-level concentration in the axial zone of the pipe (Epstein *et al.*, 1970). Roughly one quarter of the pyrochlore-supergroup minerals in Kovdor is the Na–Nb–OH mineral (Ivanyuk *et al.*, 2002), which is described herein as a hydroxynatropyrochlore, and the rest includes mainly hydroxycalciopyrochlore and U–Th-*REE*-rich hydroxykenopyrochlore (*REE* = rare-earth element), a recently approved mineral species (Miyawaki *et al.*, 2017), which was known at Kovdor previously as 'hatchettolite'. According to the previous reports (Yakovenchuk *et al.*, 2005; Subbotin and Subbotina, 2000), hydroxynatropyrochlore also occurs

Corresponding author: Sergey V. Krivovichev, Email: s.krivovichev@spbu.ru
Associate Editor: G. Diego Gatta
Cite this article: Ivanyuk G.Yu., Yakovenchuk V.N., Panikorovskii T.L., Konoplyova N., Pakhomovsky Y.A., Bazai A.V., Bocharov V.N. and Krivovichev S.V. (2019) Hydroxynatropyrochlore, $(Na,Ca,Ce)_2Nb_2O_6(OH)$, a new member of the pyrochlore group from the Kovdor phoscorite–carbonatite pipe, Kola Peninsula, Russia. *Mineralogical Magazine*, **83**, 107–113. https://doi.org/10.1180/minmag.2017.081.102

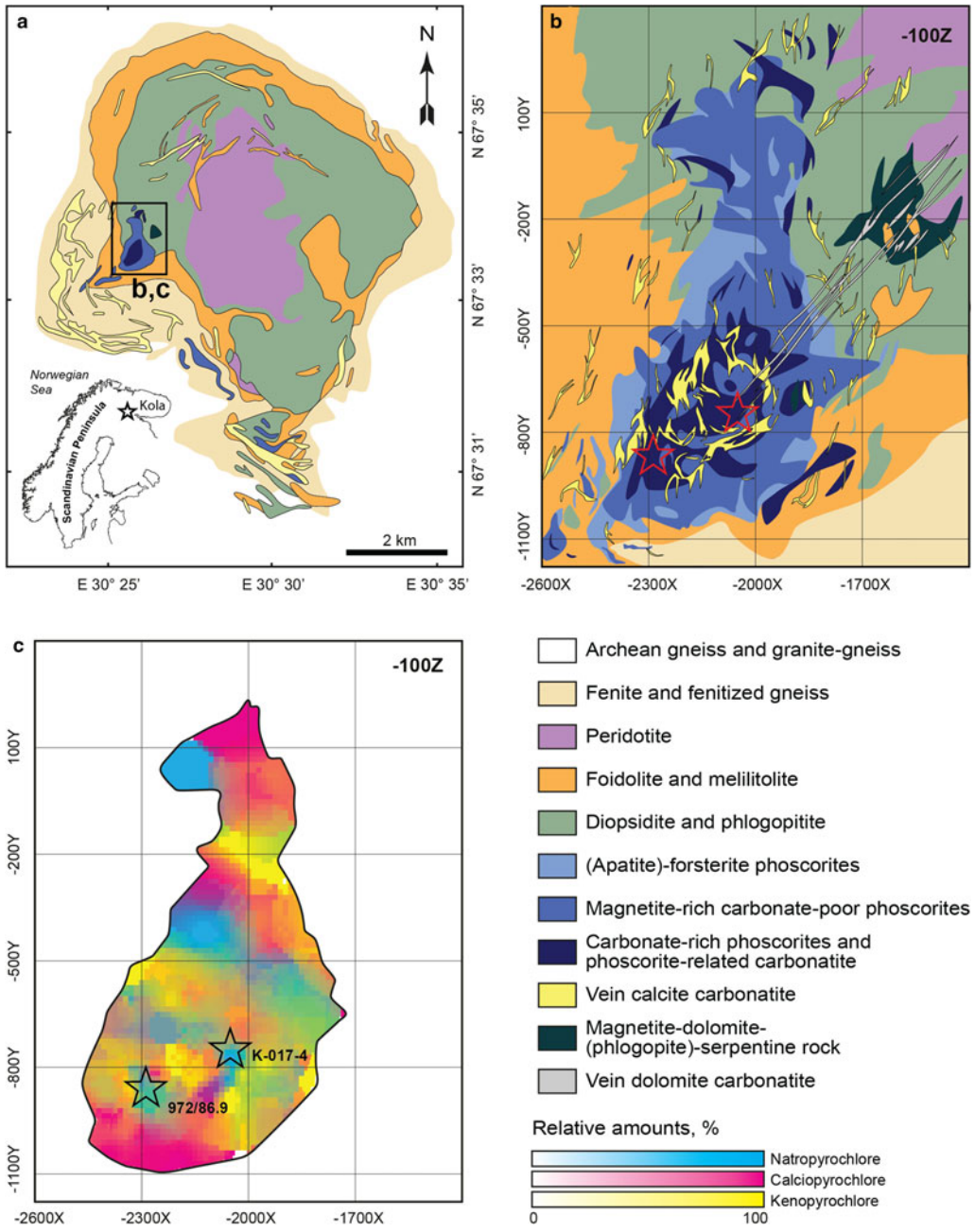

Fig. 1. Geological maps of: (*a*) the Kovdor massif (after Mikhailova *et al.*, 2016) and (*b*) the phoscorite-carbonatite pipe (after Ivanyuk *et al.*, 2016); and (*c*) distribution of relative amounts of Na-, Ca-, and vacant-dominant pyrochlores within the pipe. Stars indicate localities of holotype (972/86.9) and cotype (K-017-4) hydroxynatropyrochlore.

in Khibiny and Sebl'yavr in Murmanskaya Oblast', Russia, and other alkaline and alkaline–ultrabasic massifs. However, it has not been fully characterised (no fluorine content, structural data, etc.). Herein we report on the full characterization of the mineral, using the data obtained for the Kovdor sample.

The mineral is named in accordance with the pyrochlore supergroup nomenclature (Atencio *et al.*, 2010). The new mineral and its name were approved by the Commission on New Minerals, Nomenclature and Classification of the International Mineralogical Association (IMA2017-074, Ivanyuk *et al.*, 2017) The holotype specimen is deposited in the collections of the Mineralogical Museum of St. Petersburg State University, Russia, under catalogue number 1/19679.

Occurrence

The Kovdor massif of peridotite, foidolite, melilitolite, phoscorite, carbonatites and related metasomatic rocks (diopsidite, phlogopitite, skarn-like rocks and fenite) is a Devonian (~400 Ma, Rodionov *et al.*, 2012) volcano–plutonic complex situated within the Archean granite-gneisses in the Southwest part of the Murmansk region, Russia (67°33′N, 30°31′E). The axial part of this complex (6 km × 2 km) consists of peridotite, whereas its marginal zone (up to 1 km thick) is composed of the foidolite–melilitolite rock series (Fig. 1*a*). Intrusion of the alkaline melts at the contact between peridotite stock and host granite–gneisses caused intensive metasomatic alteration of both, with the

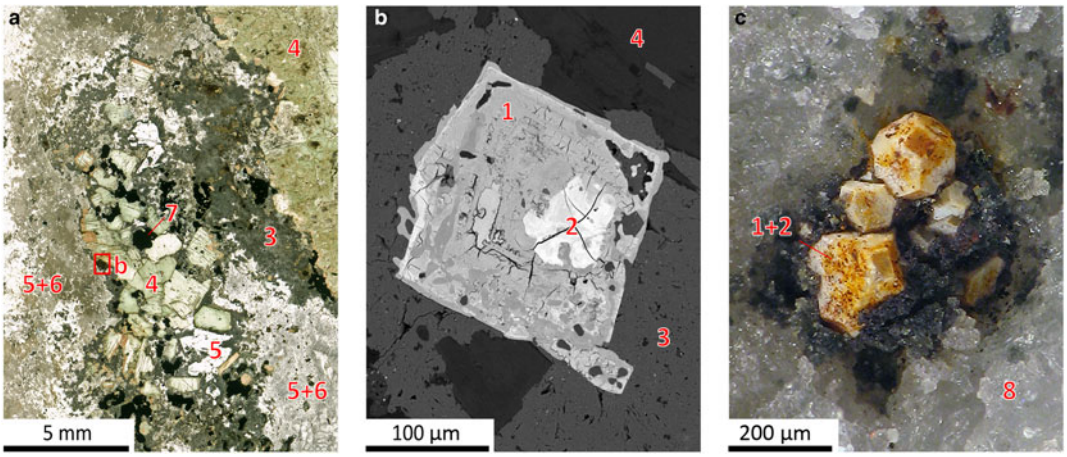

Fig. 2. Crystals of hydroxynatropyrochlore (1) in calcite carbonatite 972/86.9 (*a*, *b*) and dolomite carbonatite K-017-4 (*c*). Photo of thin section in polarised light (*a*); BSE-image (*b*); and macroscopic photo (*c*). 2 – U-rich hydroxykenopyrochlore, 3 – hydroxylapatite, 4 – phlogopite, 5 – calcite, 6 – chlorite, 7 – magnetite with ilmenite inclusions and 8 – dolomite.

formation of diopsidite, phlogopitite, melilite-, monticellite-, vesuvianite- and andradite-rich skarn-like rocks (after peridotite) and fenitised gneiss and fenite after granite–gneisses (Mikhailova *et al.*, 2016).

At the western contact of the peridotite and foidolite intrusions, there is a vertical concentrically zoned pipe of phoscorite–carbonatite rock series, with the later ring stockwork of vein calcite carbonatite and the linear zone of vein dolomite carbonatite (Fig. 1*b*). The concentric zonation of the phoscorite–carbonatite pipe is caused by the gradual transition of (apatite)–forsterite-rich phoscorite of the marginal zone into low-carbonate magnetite-rich phoscorite of the intermediate zone and then into carbonate-rich phoscorite and phoscorite-related carbonatite of the axial zone, and accented by concentration of vein calcite carbonatite approximately at the contact between the intermediate and axial zones (Mikhailova *et al.*, 2016; Ivanyuk *et al.*, 2016).

Within the phoscorite–carbonatite pipe, the content and grain sizes of the pyrochlore-group minerals gradually increase from the pipe walls towards the pipe axis (Ivanyuk *et al.*, 2016). In addition, there is a concentric zonation in distribution of calcium-, sodium- and vacancy-dominant pyrochlores (Fig. 1*c*). The marginal low-carbonate phoscorite includes only rare and tiny (up to 5 µm in diameter) grains of hydroxynatropyrochlore, while the axial carbonate-rich phoscorite and carbonatite are enriched in much larger (up to 500 µm in diameter) crystals of the same mineral. The calcite carbonatite that contains the holotype hydroxynatropyrochlore sample 972/86.9 is a fine-grained rock (Fig. 2*a*) consisting mainly of calcite (53 modal%), (tetraferri)phlogopite (30 modal%), hydroxylapatite (9 modal%) and magnetite (8 modal%). Characteristic accessory minerals include (in order of abundance): chamosite–clinochlore, ilmenite, pyrrhotite, valleriite, baddeleyite, U–Th-rich hydroxykenopyrochlore, hydroxynatropyrochlore (Fig. 2*b*), zirconolite, baryte, strontianite, chalcopyrite, galena and barytocalcite.

Hydroxynatropyrochlore also occurs in the latest dykes of dolomite carbonatite (see Fig. 1*b*) that cut through the axial carbonate-rich phoscorite and calcite carbonatite. In particular, dolomite carbonatite K-017-4 (see Fig. 1*b*,*c*) consists mainly of dolomite (85 modal%) and calcite (15 modal%) and contains numerous voids incrusted by the crystals of dolomite, calcite and magnesite overgrown by the hydroxynatropyrochlore grains (up to 300 µm in diameter, Fig. 2*c*) and compact two-zonal spherulites of gladiusite (in the core) and juonniite (in the marginal zone).

General appearance, physical and optical properties

In the phoscorite and calcite carbonatite, hydroxynatropyrochlore forms well-shaped cubic and truncated octahedral crystals (up to 700 µm in diameter) that usually contain irregularly shaped relics of amorphous U-rich hydroxykenopyrochlore (see Fig. 2*b*). In the veins of dolomite carbonatite, there are well-shaped truncated octahedral crystals of hydroxynatropyrochlore (up to 300 µm)

Table 1. Composition of holotype hydroxynatropyrochlore.

Analysis no.	1	2	Mean	S.D.*
Wt.%				
Na_2O	8.03	7.90	7.97	0.09
CaO	10.05	10.71	10.38	0.47
TiO_2	3.83	5.58	4.71	1.24
FeO	b.d.	0.83	0.42	0.59
Nb_2O_5	56.72	56.15	56.44	0.40
Ce_2O_3	3.01	4.10	3.56	0.77
Ta_2O_5	7.48	1.97	4.73	3.90
ThO_2	4.66	6.79	5.73	1.51
UO_2	3.84	3.48	3.66	0.25
H_2O_{calc}	2.31	2.49	2.37	–
F	0.09	b.d.	0.05	0.06
$-O=F_2$	−0.04	b.d.	−0.02	–
Total	99.98	100.00	100.00	
Atoms per formula unit				
Na	1.02	1.02	1.02	
Ca	0.71	0.76	0.73	
Ce	0.07	0.10	0.09	
Th	0.07	0.10	0.09	
U	0.06	0.05	0.05	
Fe^{2+}	0.00	0.05	0.02	
Sum *A*	1.93	2.08	2.00	
Nb	1.68	1.68	1.68	
Ta	0.13	0.04	0.09	
Ti	0.19	0.28	0.23	
Sum *B*	1.97	2.00	2.00	
O	5.96	6.09	6.03	
OH	1.01	1.10	1.04	
F	0.02	0.00	0.01	
Sum *Y*	1.03	1.10	1.05	

*S.D. = standard deviation; b.d. = below detection limit.

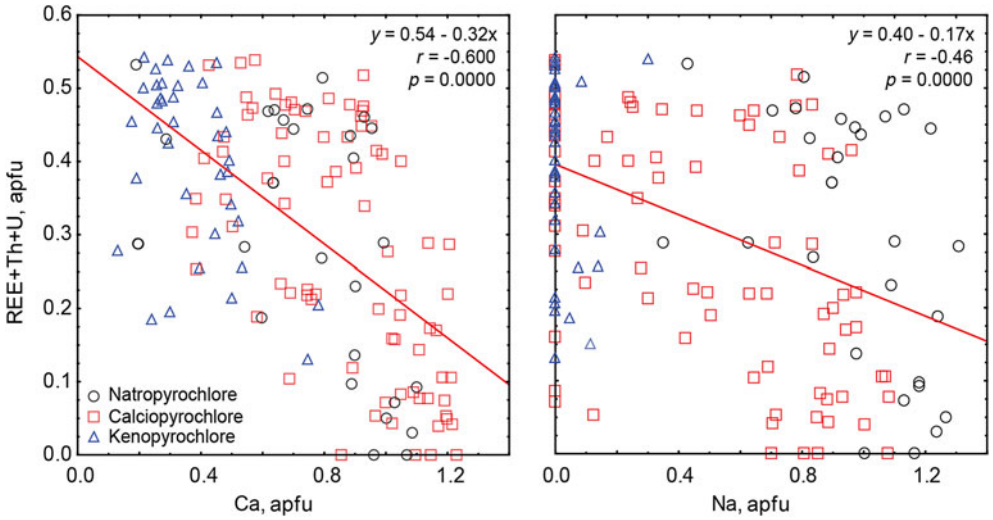

Fig. 3. Relation between contents of Ca, Na and high-valent cations in the *A*-position of the pyrochlore-supergroup minerals from the Kovdor phoscorite–carbonatite pipe. Legend: *y* is the total content of *REE*, Th and U, *x* is the content of Ca (*left*) or Na (*right*), *r* and *p* are correlation coefficient and probability value at 95% level of significance, respectively.

with a thin (up to 50 μm) marginal zone of U-rich hydroxykenopyrochlore (see Fig. 2*c*).

Hydroxynatropyrochlore is brittle and has a conchoidal fracture. The cleavage is average on {111}. No twinning or parting were observed. The Mohs hardness is ~5. The density, determined by the sink–float method in Clerici solution, is 4.60(5) g cm^{-3}, and the calculated density is 4.77 g cm^{-3} (using the empirical formula and single-crystal unit-cell parameters). The observed difference is most probably due to the admixtures of hydroxykenopyrochlore.

Macroscopically, hydroxynatropyrochlore is pale brown, with an adamantine to greasy lustre. The crystals are translucent to transparent, with a white streak. The mineral is isotropic, with the refractive index $n = 2.10(5)$ at 589 nm. The mineral is non-fluorescent. A Gladstone-Dale calculation provides a compatibility index of 0.028 (with the empirical formula and single-crystal XRD data), which is regarded as excellent (Mandarino, 1981).

Chemical composition

The chemical composition of hydroxynatropyrochlore was determined by wavelength-dispersive spectrometry using a Cameca MS-46 electron microprobe (at the Geological Institute, Kola Science Centre, Russian Academy of Sciences, Apatity) operating at 20 kV, 20–30 nA, with a 10 μm beam diameter. The standards used were: lorenzenite (Na and Ti), diopside (Ca), hematite (Fe), thorite (Th), synthetic $LaCeS_2$ (Ce), and also metallic Nb, Ta and U. The fluorine content was determined using a LEO-1450 scanning electron microscope with a Quantax energy-dispersive microanalyser using fluorapatite as a standard. The water content was not determined due to the intimate intergrowth of hydroxynatropyrochlore and U–Ta-rich water-bearing hydroxykenopyrochlore. It was estimated from the weight deficit, whereas the presence of OH groups and absence of molecular water were confirmed by the Raman spectroscopy.

Analytical results for the structurally characterised holotype hydroxynatropyrochlore 972/86.9 are provided in Table 1 (see Figs 1*c* and 2*b*). The average chemical composition of the mineral corresponds to the following empirical formula (calculated on the basis of Nb + Ta + Ti = 2): $(Na_{1.02}Ca_{0.73}Ce_{0.09}Th_{0.09}U_{0.05}Fe^{2+}_{0.02})_{\Sigma 2.00}(Nb_{1.68}Ti_{0.23}Ta_{0.09})_{\Sigma 2.00}O_{6.03}(OH_{1.04}F_{0.01})_{\Sigma 1.05}$. The simplified general formula is $(Na,Ca,Ce)_2Nb_2O_6(OH)$.

In the pyrochlore-supergroup minerals of the Kovdor phoscorite–carbonatite complex, both Na and Ca contents decrease with the increase in the total content of high-valent cations (Fig. 3), though the slope of the Ca-plot is steeper. This indicates that, most probably, natropyrochlore is a result of the complex substitution of Ca^{2+} by REE^{3+}, Th^{4+} and U^{4+} (±Na^{+} and □) in the Na–Ca pyrochlore series, $(NaCa)Nb_2O_6(OH,F)$: $NaCa \leftrightarrow NaCa_{0.7}REE_{0.2}\square_{0.1}$, $NaCa \leftrightarrow NaCa_{0.5}(Th,U)_{0.25}\square_{0.25}$, $NaCa \leftrightarrow Na_{1.5}REE_{0.5}$ and $NaCa \leftrightarrow Na_{1.6}(Th,U)_{0.1}\square_{0.3}$. The increase of the total (U + Th) content above 20 wt.% results in the metamictisation of the mineral, the loss of Na and Ca, the increase of the H_2O content, and the transformation of the mineral into hydroxykenopyrochlore. The F content in 'natropyrochlores' varies randomly from zero to 0.51 apfu. (atoms per formula unit), so a small portion of the samples investigated corresponds to fluornatropyrochlore.

Hydroxynatropyrochlore dissolves slowly in hot HCl, and this process is activated by the mineral metamictisation due to the high contents of U and Th.

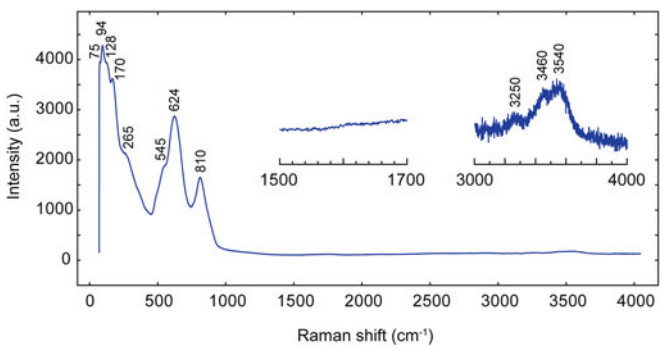

Fig. 4. Raman spectrum of hydroxynatropyrochlore 972/86.9.

Table 2. Raman shifts in the hydroxynatropyrochlore spectrum and their assignment.

Shift, cm^{-1}	Group	Type
75sh, 94, 128sh, 170	*A*, *B*	Lattice vibrations
265sh	BO_6	Bending modes
545sh, 624	BO_6	Stretching modes
810	*B*–O	Stretching modes
3250, 3460, 3540	O–H	Stretching modes

sh – shoulder.

Table 3. Data collection information and structure-refinement parameters for hydroxynatropyrochlore.

Crystal data	
Temperature (K)	293(2)
Crystal system	Cubic
Space group	$Fd\bar{3}m$
a (Å)	10.3276(5)
Volume ($Å^3$)	1101.52(17)
Z	8
Calculated density ($g\ cm^{-3}$)	4.77
Data collection	
Diffractometer	Bruker Kappa APEX DUO
Absorption correction	*APEX 2* (Bruker-AXS, 2014)
μ (mm^{-1})	5.645
F(000)	1385.0
Crystal size (mm^3)	0.14 × 0.14 × 0.14
Radiation	Mo*Kα* (λ = 0.71073)
2θ range (°)	6.834 to 54.988
T_{min}, T_{max}	0.440, 1.000
Index ranges	$-12 \le h \le 13$, $-13 \le k \le 6$, $-12 \le l \le 13$
Reflections collected	1819
Independent reflections	80 [R_{int} = 0.0222, R_{sigma} = 0.0053]
Refinement	
Data/restraints/parameters	80/0/12
Goodness-of-fit on F^2	1.352
Final *R* indices [$I > 2\sigma(I)$]	R_1 = 0.0265, wR_2 = 0.0688
Final *R* indices [all data]	R_1 = 0.0280, wR_2 = 0.0709
Largest diff. peak/hole, e^- $Å^{-3}$	0.67/–0.34

Raman spectroscopy

The Raman spectrum of holotype hydroxynatropyrochlore (Fig. 4) was obtained using a Horiba Jobin-Yvon LabRam HR 800 spectrometer (wavelength 514 nm). The assignments of the absorption bands have been made by analogy with other pyrochlore-like compounds (Bahfenne and Frost 2010; Mączka *et al.*, 2012) and are given in Table 2. In the spectrum, there are weak bands of the ν_1 stretching vibrations of hydroxyl groups, and there are no characteristic bands of the H_2O vibrations at 1600 cm^{-1}.

Crystal structure

Experimental

Single-crystal X-ray diffraction of the holotype hydroxynatropyrochlore 972/86.9 was performed at 293 K using a Bruker Kappa APEX DUO diffractometer equipped with an IμS microfocus source (beam size of 0.11 mm) operated at 45 kV and 0.6 mA and a CCD area detector, by means of monochromated Mo*Kα* radiation (λ = 0.71073 Å). The intensity data were reduced and corrected for Lorentz, polarisation and background effects. A multi-scan absorption-correction was applied by the Bruker software *APEX2* (Bruker-AXS, 2014). The crystal structure was refined with the *SHELX* program (Sheldrick, 2008) in the $Fd\bar{3}m$ space group to R_1 = 0.026 (R_{int} = 0.0222) for 80 independent reflections with $F_o > 4\sigma(F_o)$. The crystal structure was drawn using the *VESTA 3* program (Momma and Izumi, 2011). The scattering factors were calculated from the initial model using the Ca- and Na-scattering curves for the *A* site, the Nb- and Ti-scattering curves for the *B* site, and the O-scattering curves for other sites. All cation site occupancies are given in accordance with the electron-microprobe data (normalised on the basis of two *B* cations per formula unit). Crystal data, data collection information and structure refinement details are given in Table 3, atom coordinates and displacement parameters are listed in Table 4, and selected interatomic distances are provided in Table 5. The crystallographic information files have been deposited with the Principal Editor of *Mineralogical Magazine* and are available as Supplementary material (see below).

Table 5. Selected interatomic distances in the crystal structure of hydroxynatropyrochlore.

*B*1–O1	1.958(2) ×6
*A*1–1	2.2360(1) ×2
*A*1–O1	2.616(5) ×6
<*A*1–O>	2.521

Results

The crystal structure of hydroxynatropyrochlore (Fig. 5) belongs to the pyrochlore structure type with the ideal formula $A_2B_2O_6Y_1$ (Atencio *et al.*, 2010). It can be described as a three-dimensional octahedral framework of corner-sharing BO_6 octahedra with *A* cations and OH groups in the interstices (Gargori *et al.*, 2010; Yin *et al.*, 2015).

The calculated site-scattering factor for the *A* site is 18.4 epfu (electrons pfu), which is somewhat smaller than the value of 19.6 epfu derived from electron-microprobe data, probably due to the variable U content in different zones of the crystal studied. The *A* (16*c*) site is occupied predominately by Na, and its final occupancy can be given as $(Na_{0.51}Ca_{0.35}\square_{0.04}U_{0.03}Th_{0.035}Ce_{0.035})_{\Sigma 1.00}$. The octahedral *B* (16*d*) site has the site-scattering factor of 40.2 epfu, which agrees quite well with the assigned occupancy of $(Nb_{0.84}Ti_{0.095}Ta_{0.065})_{1.00}$ (41.3 epfu). The O1 (48*f*) and *Y*1 (8*a*) sites are occupied by O and OH, respectively. The crystal chemical formula of the holotype hydroxynatropyrochlore can be written as

Table 4. Atom coordinates, displacement parameters ($Å^2$), site occupancies and site-scattering factors (SSFs, in epfu) for hydroxynatropyrochlore.

Site	Occupancy	*x*	*y*	*z*	U_{eq}	SSF_{str}	SSF_{chem}	U^{11}	U^{22}	U^{33}	U^{12}	U^{13}	U^{23}
*B*1	$Nb_{0.84}Ti_{0.095}Ta_{0.065}$	0	½	0	0.018(1)	40.2	41.3	0.0183(5)	= U^{11}	= U^{11}	−0.0015(3)	= U^{12}	= U^{12}
*A*1	$Na_{0.51}Ca_{0.35}\square_{0.04}Th_{0.035}Ce_{0.035}U_{0.03}$	¾	¾	0	0.030(2)	18.4	19.6	0.0300(15)	= U^{11}	= U^{11}	0.0037(8)	= U^{12}	= U^{12}
*Y*1	OH	⅝	⅝	⅛	0.045(5)	8.0	8.0	0.045(5)	= U^{11}	= U^{11}	0	0	0
O1	$O_{0.993}OH_{0.007}$	−0.0685(6)	⅝	⅛	0.024(2)	8.0	8.0	0.027(4)	0.023(2)	= U^{22}	−0.008(3)	0	0

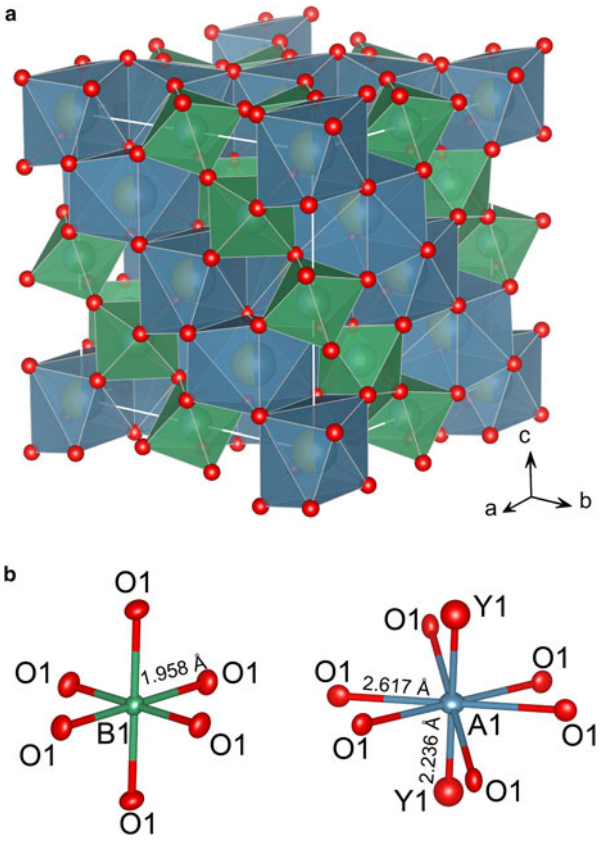

Fig. 5. A general view of crystal structure of hydroxynatropyrochlore: (*a*) in cation-centred polyhedral representation (AO_8 polyhedra are blue, BO_6 octahedra are green, oxygen sites shown as red spheres); and (*b*) coordination environments of the *A* and *B* sites. Displacement ellipsoids are drawn at the 50% probability level.

$(Na_{1.02}Ca_{0.70}\square_{0.08}Ce_{0.07}Th_{0.07}U_{0.06})_{\Sigma 2.00}(Nb_{1.68}Ti_{0.19}Ta_{0.13})_{\Sigma 2.00}[O_{5.96}OH_{0.04}]_{\Sigma 6.00}(OH)_{1.00}$, which is in good agreement with the empirical formula.

Powder X-ray diffraction

The powder X-ray diffraction pattern of the sample 972/86.9 (Table 6) was obtained using a Rigaku R-AXIS RAPID II diffractometer equipped with a cylindrical image plate detector using the Debye-Scherrer geometry (d = 127.4 mm; Co$K\alpha$ radiation). The data were integrated using the *Osc2Tab/SQRay* software (Britvin *et al.*, 2017). The unit-cell parameters refined from the powder data are as follows: $Fd\bar{3}m$, a = 10.3211(3) Å, V = 1099.46(8) Å^3 and Z = 8, which are in good agreement with the single-crystal data (see Table 3).

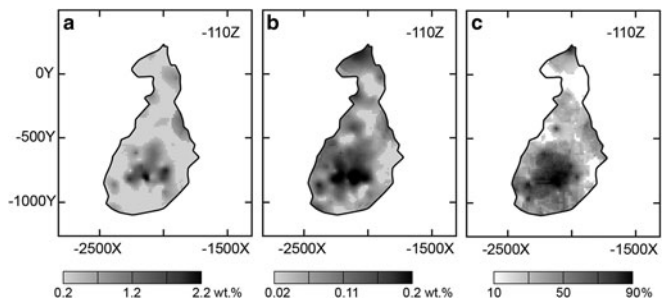

Fig. 6. Relation between the contents of Sc (*a*) and Nb (*b*) in baddeleyite and the occurrence of the pyrochlore-supergroup-bearing rocks (*c*) in the Kovdor phoscorite–carbonatite pipe.

Table 6. Powder X-ray diffraction data for hydroxynatropyrochlore*.

I_{obs}	I_{calc}	d_{obs}, Å	d_{calc}, Å	*h k l*
47	**72**	**5.96**	**5.96**	**1 1 1**
30	**31**	**3.110**	**3.112**	**3 1 1**
100	**100**	**2.580**	**2.580**	**2 2 2**
19	**16**	**2.368**	**2.368**	**4 0 0**
1	3	2.107	2.107	4 2 2
6	**5**	**1.9875**	**1.9863**	**3 3 3**
25	**18**	**1.8257**	**1.8245**	**4 4 0**
3	2	1.7458	1.7446	5 3 1
0.5	1	1.6322	1.6319	6 2 0
2	2	1.5737	1.5739	5 3 3
14	**8**	**1.5561**	**1.5559**	**6 2 2**
3	2	1.4899	1.4897	4 4 4
2	3	1.4453	1.4452	5 5 1
2	4	1.3438	1.3437	7 3 1
2	3	1.2902	1.2901	8 0 0
0.5	1	1.2164	1.2163	8 2 2
0.5	1	1.1916	1.1917	7 5 1
2	2	1.1840	1.1839	6 6 2
2	2	1.1540	1.1539	8 4 0
0.5	3	1.1329	1.1328	9 1 1
0.5	2	1.0821	1.0819	9 3 1
1	1	1.0535	1.0534	8 4 4
0.5	1	1.0375	1.0373	7 5 5
0.5	1	1.0116	1.0120	10 2 0
1	2	0.9975	0.9977	9 5 1

*The strongest lines are highlighted in bold.

Discussion

In the Kovdor phoscorite–carbonatite pipe, there was an intensive hydrothermal alteration of primary minerals, with the formation of numerous secondary phases: clinochlore or glagolevite after phlogopite, clinohumite and serpentine after forsterite, pyrochlore and zirconolite after baddeleyite, etc. (Mikhailova *et al.*, 2016; Ivanyuk *et al.*, 2002, 2016). The higher content of Nb and Sc in baddeleyite from the axial carbonate-rich phoscorite and carbonatite due to the $2Zr^{4+} \leftrightarrow Sc^{3+} + Nb^{5+}$ substitution results in the intensive replacement of this mineral by pyrochlore-supergroup minerals (Fig. 6) accompanied by the formation of Sc phosphates (Yakovenchuk *et al.*, 2018):

$$24Bdy' + 12Dol + 8Ap + 56H_2O + 10CO_2 + 6Na^+ = 6Pcl + 34Cal + 12Jnn + 3H_2,$$

where Ap = hydroxylapatite; Bdy' = Sc–Nb end-member of baddeleyite, $Sc_{0.5}Nb_{0.5}O_2$; Cal = calcite, Dol = dolomite; Jnn = juonniite, $CaMgScP_2O_8(OH)\cdot 4H_2O$; and Pcl = pyrochlore-supergroup member with formula $NaCaNb_2O_6(OH)$.

Thus, in the Kovdor phoscorite–carbonatite complex, members of the pyrochlore supergroup are secondary hydrothermal minerals resulting mainly from the alteration of Nb-rich baddeleyite. Hydroxynatropyrochlore itself originates from the hypothetical Na–Ca pyrochlore, $NaCaNb_2O_6(OH)$, due to preferential substitution of Ca by *REE*, Th and U. The increase of the U and Th contents results in its metamictisation. In addition, at the latest stage of the phoscorite–carbonatite pipe formation, an insignificant part of hydroxynatropyrochlore transforms into fluornatropyrochlore with the approximately equal contents of F and OH, by analogy with accompanied transition of hydroxylapatite into fluorapatite (Ivanyuk *et al.*, 2016).

Supplementary material. To view supplementary material for this article, please visit https://doi.org/10.1180/minmag.2017.081.102

Acknowledgements. We thank P. Leverett, D. Atencio and an anonymous reviewer for useful remarks. Authors are grateful to Drs A.O. Kalashnikov, J.A. Mikhailova and V.A. Sokharev for the co-operation in the geological study of the Kovdor phoscorite–carbonatite complex. The research is supported by the Russian Science Foundation, grant 16-17-10173. X-ray diffraction studies were undertaken at the XRD Research Resource Centre of St. Petersburg State University.

References

Andrade M., Atencio D., Persiano A. and Ellena J. (2013) Fluorcalciomicrolite, $(Ca,Na,\square)_2Ta2O6F$, a new microlite-group mineral from Volta Grande pegmatite, Nazareno, Minas Gerais, Brazil. *Mineralogical Magazine*, **77**, 2989–2996.

Andrade M., Atencio D., Chukanov N. and Ellena J. (2015) Hydrokenomicrolite, $(\square,H_2O)_2Ta_2(O,OH)_6(H_2O)$, a new microlite-group mineral from Volta Grande pegmatite, Nazareno, Minas Gerais, Brazil. *American Mineralogist*, **98**, 292–296.

Andrade M.B., Yang H., Atencio D., Downs R.T., Chukanov N.V., Lemée-Cailleau M.H., Persiano A.I.C., Goeta A.E. and Ellena J. (2016) Hydroxycalciomicrolite, $Ca_{1.5}Ta_2O_6(OH)$, a new member of the microlite group from Volta Grande pegmatite, Nazareno, Minas Gerais, Brazil. *Mineralogical Magazine*, **81**, 555–564.

Atencio D., Andrade M.B., Christy A.G., Gieré R. and Kartashov P.M. (2010) The pyrochlore supergroup of minerals nomenclature. *The Canadian Mineralogist*, **48**, 673–698.

Atencio D., Ciriotti M.E. and Andrade M.B. (2013) Fluorcalcioroméite, $(Ca,Na)_2Sb_2^{5+}(O,OH)_6F$, a new roméite-group mineral from Starlera mine, Ferrera, Grischun, Switzerland: description and crystal structure. *Mineralogical Magazine*, **77**, 467–473.

Atencio D., Andrade M.B., Bastos Neto A.C. and Pereira V.P. (2017) Ralstonite renamed hydrokenoralstonite, coulsellite renamed fluornatrocoulsellite, and their incorporation into the pyrochlore supergroup. *The Canadian Mineralogist*, **55**, 115–120.

Bahfenne S. and Frost R.L. (2010) Raman spectroscopic study of the antimonate mineral roméite. *Spectrochimica Acta A*, **75**, 637–639.

Biagioni C., Orlandi P., Nestola F. and Bianchin S. (2013) Oxycalcioroméite, $Ca_2Sb_2O_6O$, from Buca della Vena mine, Apuan Alps, Tuscany, Italy: a new member of the pyrochlore supergroup. *Mineralogical Magazine*, **77**, 3027–3037.

Britvin S.N., Dolivo-Dobrovolsky D.V. and Krzhizhanovskaya M.G. (2017) Software for processing of X-ray powder diffraction data obtained from the curved image plate detector of Rigaku RAXIS Rapid II diffractometer. *Zapiski Rossiiskogo Mineralogicheskogo Obshestva*, **146**(3), 104–107 [in Russian].

Bruker-AXS (2014) *APEX2*. Version 2014.11-0. Madison, Wisconsin, USA.

Christy A.G. and Atencio D. (2013) Clarification of status of species in the pyrochlore supergroup. *Mineralogical Magazine*, **77**, 13–20.

Epstein E.M., Basmanov V.N., Berezina L.A., Gol'dfurt T.L., Zhuravleva L.N., Nechaeva E.A., Sokolov S.V. and Chernyshova L.V. (1970) *The appropriateness of allocation, the mineralogical and geochemical features and valuation of iron-phosphorus and rare-metal ores of the Kovdor deposit*. Report about scientific works. Vol.1. Moscow, Russia (Archives of the Geological Institute of the Kola Science Centre of RAN) 217 pp. [in Russian].

Fan G., Ge X., Li G., Yu A. and Shen G. (2016) Oxynatromicrolite, $(Na,Ca,U)_2Ta_2O_6(O,F)$, a new member of the pyrochlore supergroup from Guanpo, Henan Province, China. *Mineralogical Magazine*, **81**, 743–751.

Gargori C., Galindo R., Cerro S., García A., Llusar M. and Monrós G. (2010) Synthesis of a new $Ca_xY_{2-x}V_xSn_{2-x}O_7$ yellow pigment. *Physics Procedia*, **8**, 84–87.

Hålenius U. and Bosi F. (2013) Oxyplumboroméite, $Pb_2Sb_2O_7$, a new mineral species of the pyrochlore supergroup from Harstigen mine, Värmland, Sweden. *Mineralogical Magazine*, **77**, 2931–2939.

Ivanyuk G.Yu., Yakovenchuk V.N. and Pakhomovsky Ya.A. (2002) *Kovdor*. Laplandia Minerals, Apatity, 326 pp.

Ivanyuk G.Yu., Kalashnikov A.O., Pakhomovsky Ya.A., Mikhailova J.A., Yakovenchuk V.N., Konopleva N.G., Sokharev V.A., Bazai A.V. and Goryainov P.M. (2016) Economic minerals of the Kovdor baddeleyite-apatite-magnetite deposit, Russia: mineralogy, spatial distribution, and ore processing optimization. *Ore Geology Reviews*, **77**, 279–311.

Ivanyuk G.Y., Yakovenchuk V.N., Panikorovskii T.L., Konoplyova N., Pakhomovsky Y.A., Bazai A.V., Bocharov V.N. and Krivovichev S.V. (2017) Hydroxynatropyrochlore, IMA 2017-074. CNMNC Newsletter No. 40, December 2017, page 1580; *Mineralogical Magazine*, **81**, 1577–1581.

Jingwu Y., Li G., Guangming Y., Ge X., Xu H. and Wang J. (2015) Fluornatropyrochlore, a new pyrochlore supergroup mineral from the Boziguoer rare earth element deposit, Baicheng County, Akesu, Xinjiang, China. *The Canadian Mineralogist*, **53**, 455–460.

Kalashnikov A.O., Yakovenchuk V.N., Pakhomovsky Y.A., Bazai A.V., Sokharev V.A., Konopleva N.G., Mikhailova J.A., Goryainov P.M. and Ivanyuk G.Yu. (2016) Scandium of the Kovdor baddeleyite–apatite–magnetite deposit (Murmansk Region, Russia): Mineralogy, spatial distribution, and potential resource. *Ore Geology Reviews*, **72**, 532–537.

Li G., Yang G., Lu F., Xiong M., Ge X., Pan B. and de Fourestier J. (2016) Fluorcalciopyrochlore, a new mineral species from Bayan Obo, Inner Mongolia, P.R. China. *The Canadian Mineralogist*, **54**, 1285–1291.

Mączka M., Knyazev A.V., Kuznetsova N.Yu., Ptak M. and Macalik L. (2011) Raman and IR studies of $TaWO_{5.5}$, $ASbWO_6$ (A = K, Rb, Cs, Tl) and $ASbWO_6{\cdot}H_2O$ (A = H, NH_4, Li, Na) pyrochlore oxides. *Journal of Raman Spectroscopy*, **42**, 529–533.

Mandarino J.A. (1981) The Gladstone – Dale relationship: Part IV. The compatibility concept and its application. *The Canadian Mineralogist*, **19**, 441–450.

Mikhailova J.A., Kalashnikov A.O., Sokharev V.A., Pakhomovsky Y.A., Konopleva N.G., Yakovenchuk V.N., Bazai A.V., Goryainov P.M. and Ivanyuk G.Y. (2016) 3D mineralogical mapping of the Kovdor phoscorite–carbonatite complex (Russia). *Mineralium Deposita*, **51**, 131–149.

Mills S.J., Christy A.G., Kampf A.R., Birch W.D. and Kasatkin A. (2017) Hydroxykenoelsmoreite, the first new mineral from the Republic of Burundi. *European Journal of Mineralogy*, **29**, 491–497.

Miyawaki R., Momma K., Matsubara S., Sano T., Shigeoka M. and Horiuchi H. (2017) Hydroxykenopyrochlore, IMA 2017-030a. CNMNC Newsletter No. 39, October 2017. *Mineralogical Magazine*, **81**, 1285.

Momma K. and Izumi F. (2011) VESTA 3 for three-dimensional visualization of crystal, volumetric and morphology data. *Journal of Applied Crystallography*, **44**, 1272–1276.

Rodionov N.V., Belyatsky B.V., Antonov A.V., Kapitonov I.N. and Sergeev S.A. (2012) Comparative in-situ U–Th–Pb geochronology and trace element composition of baddeleyite and low-U zircon from carbonatites of the Palaeozoic Kovdor alkaline–ultramafic complex, Kola Peninsula, Russia. *Gondwana Research*, **21**, 728–744.

Sheldrick G.M. (2008) A short history of SHELX. *Acta Crystallographica*, **A64**, 112–122.

Subbotin V.V. and Subbotina G.F. (2000) Minerals of the pyrochlore group in phoscorites and carbonatites of the Kola Peninsula. *Vestnik MGTU*, **3**(2), 273–284 [in Russian].

Yakovenchuk V.N., Ivanyuk G.Yu., Pakhomovsky Ya.A. and Men'shikov Yu.P. (2005) *Khibiny*. Laplandia Minerals, Apatity, 2005. 468 pp.

Yakovenchuk V.N., Ivanyuk G.Y., Pakhomovsky Y.A., Panikorovskii T.L., Britvin S.N., Krivovichev S.K., Shilovskikh V.V. and Bocharov V.N. (2018) Kampelite, $Ba_3Mg_{1.5}Sc_4(PO_4)_6(OH)_3{\cdot}4H_2O$, a new very complex Ba-Sc phosphate mineral from the Kovdor phoscorite-carbonatite complex (Kola Peninsula, Russia). *Mineralogy and Petrology*, **112**, 111–112.

Witzke T., Steins M., Doering T., Schuckmann W., Wegner R. and Pöllmann H. (2011). Fluornatromicrolite, $(Na,Ca,Bi)_2Ta_2O_6F$, a new mineral species from Quixaba, Paraiba, Brazil. *The Canadian Mineralogist*, **49**, 1105–1110.

Yang G., Li G., Xiong M., Pan B. and Yan C. (2014) Hydroxycalciopyrochlore, a new mineral species from Sichuan, China. *Acta Geologica Sinica, English Edition*, **88**, 748–753.

Yin J., Li G., Yang G., Ge X., Xu H. and Wang J. (2015) Fluornatropyrochlore, a new pyrochlore supergroup mineral from the Boziguoer rare earth element deposit, Baicheng county, Akesu, Xinjiang, China. *The Canadian Mineralogist*, **53**, 455–460.